

The Effect of welding method and heat treatment on creep resistance of Inconel 718 sheet welds

Zenon A. Opiekun¹, Agnieszka Jędrusik²

Rzeszów University of Technology, Department of Foundry and Welding, Al. Powstańców Warszawy, Poland

Abstract— The paper presents results of a study on the effect of welding technique and heat treatment on structure and creep resistance of welded joints made on thin (0.5–1.2 mm) Inconel 718 sheet with the use of GTAW and laser method without filler metal. Technological high-temperature creep tests consisted in measuring the time to rupture for sheet metal without and with welded joints under constant stress $\sigma = 150 \text{ MPa}$ and at constant temperature $t_c = (860 \pm 2)^\circ\text{C}$.

Sheet metal joints made with the use of GTAW method and laser-welded are characterized with a three-zone macrostructure, including the weld with size of dendritic grains depending on welding method, the heat-affected zone (HAZ), and the base material (BM). For GTAW method, with increasing sheet metal thickness, the observed values of parameter λ_{2s} (distance between axes of second-order branches of dendritic grains) decrease from about 12 μm to 8 μm , and similarly, in case of laser welding, λ_{2s} values decrease from about 9.6 μm to 5 μm with increasing sheet metal thickness.

Thin sheet Inconel 718 in as-delivered condition high-temperature creep-tested have the time to rupture on the level of 12 h at elongation of about 48%. Similar time-to-rupture values characterize the joints made by laser welding. GTAW joints are characterized by about 30% shorter time to rupture and elongation less by about 45%.

The microstructure change induced by heat treatment (solution treatment and two-stage ageing) resulted in significant increase of creep resistance properties of both base metal and laser-welded joints. The time to rupture of heat-treated specimens of thin Inconel 718 sheet and laser-welded joints creep-tested at $860^\circ\text{C} \pm 2^\circ\text{C}$ under stress of 150 MPa was about 19.5 h with elongation ranging from 23% to 33%.

Keywords— Inconel 718, GTAW, laser welding, heat treatment, microstructure, high-temperature creep.

I. INTRODUCTION

Inconel 718, a nickel-based alloy, belongs to a large group of heat-resisting and creep-resisting metallic materials used to manufacture a variety of welded structures, especially in aircraft industry where they are used for exhaust components in PW400 and CF6 jet engines [1–4]. The alloy shows good weldability and can be heat-treated by precipitate strengthening [5–9]. Components made of thin Inconel 718 sheet can work at high temperatures which in case of combustion chambers can reach 1300°C [2, 8].

In operating conditions, welded structures with components made of the alloy are subject to both high temperatures and large stresses. In view of the above, creep-resisting properties of welded joints in such structures are of great importance.

The sources of concentrated heat streams used to weld Inconel 718 sheet include: electric arc in GTAW welding method [10–12] and a beam of monochromatic light in case of laser welding.

The paper concerns the effect of the two welding methods used for welding thin Inconel 718 sheet [13, 14] and heat treatment on structure and the time to rupture of obtained joints measured in high-temperature creep test.

II. MATERIAL AND METHODOLOGY

The material used in the study was thin Inconel 718 alloy sheet with thickness 0.5 mm, 0.9 mm, and 1.2 mm. Chemistry of each material type was determined with the use of emission spectrometer Q4 TASMAN (Bruker). Table 1 summarizes average chemical composition of the examined sheet metal samples.

TABLE 1

CHEMISTRY OF 0.5-mm, 0.9-mm, and 1.2-mm THICK INCONEL 718 SHEET SPECIMENS USED IN THE STUDY (AVERAGE FROM 5 MEASUREMENTS FOR EACH SHEET THICKNESS).

Sheet thickness (mm)	Alloy components (% wt.)										
	Cr	Fe	Nb	Mo	Ti	Al	Si	C	B	N	Ni
0.5	17.30	16.20	5.20	2.45	1.0	0.55	0.16	0.050	0.022	0.040	balance
0.9	17.20	16.30	5.25	2.50	1.20	0.57	0.17	0.061	0.021	0.038	balance
1.2	17.28	16.15	5.30	2.38	1.18	0.54	0.14	0.059	0.023	0.041	balance

For the purpose of the study, sheet alloy specimens were prepared with joints arc-welded by means of GTAW methods and with joints obtained with the use of monochromatic light beam generated by TruLaser Robot 5020 (TRUMPF). Heat treatment of thin sheet metal specimens with welded joints was carried out in Nabertherm N 61/H electric chamber furnace according to schematic diagram shown in Fig. 1.

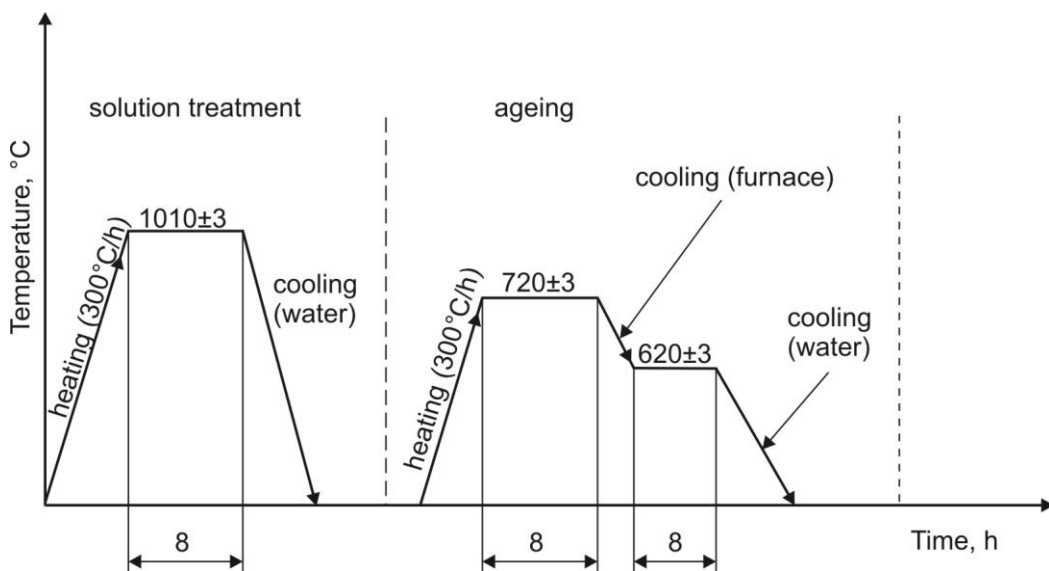


FIG. 1 — SCHEMATIC DIAGRAM REPRESENTING THE COURSE OF HEAT TREATMENT APPLIED TO THIN INCONEL 718 SHEET WITH GTAW AND LASER JOINTS.

The sheet metal was arc-welded in argon atmosphere according to GTAW method or laser-welded. Based on results of visual inspection, the best welds were identified and corresponding parameters of welding were adopted in further analysis. The best GTAW joints were obtained when welding parameters were $I = 20$ A/80 ms, 30 A/80 ms, and 40 A/80 ms for 0.5-mm, 0.9-mm, and 1.2-mm thick sheet metal, respectively. The welding rate $V_{GTAW} = 200$ mm/min was the same for all sheet grades, with arc length $\tau_A = 3$ mm; diameter of non-consumable electrode (W + 2% Y₂O₃) sharpened at angle 45° was $\varnothing = 2.4$ mm, and consumption of argon with purity 99.95% Ar was 8 L/min.

Similarly, the following parameters were adopted for further studies concerning laser welding of thin Inconel 718 sheet: welding rate $V_L = 300$ mm/min; focal length $f_l = 340$ mm; laser power $P = 690$ W, 780 W, and 990 W for 0.5-mm, 0.9-mm, and 1.2-mm thick sheet metal, respectively.

Examination of creep resistance of welded joints in thin Inconel 718 sheet consisted in determining their time to rupture in the course of technological high-temperature creep tests under conditions of constant stress $\sigma = 150$ MPa and constant temperature $t_c = (860 \pm 2)^\circ\text{C}$ [15]. For the purpose of this study, specimens (Fig. 2) with $\varnothing 8$ mm holes in the holder portion were prepared. The specimens were fixed in holders by means of $\varnothing 8$ mm mandrels (Fig. 3). Holders and mandrels were made of creep-resistant cobalt-based alloy MAR-M509 [16].

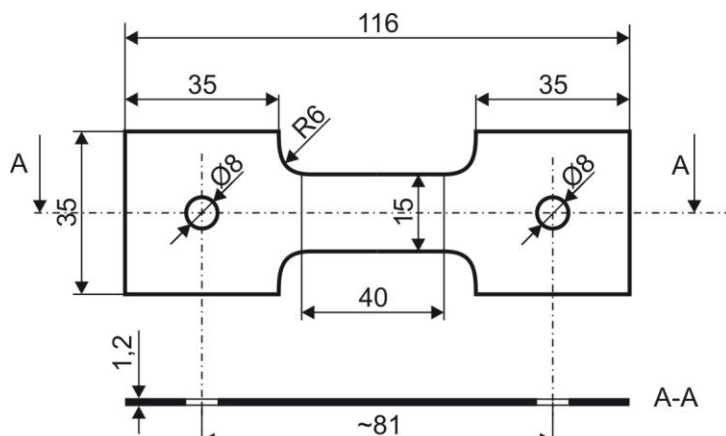


FIG. 2 — AN EXAMPLE SPECIMEN USED FOR HIGH-TEMPERATURE CREEP RESISTANCE TESTS.

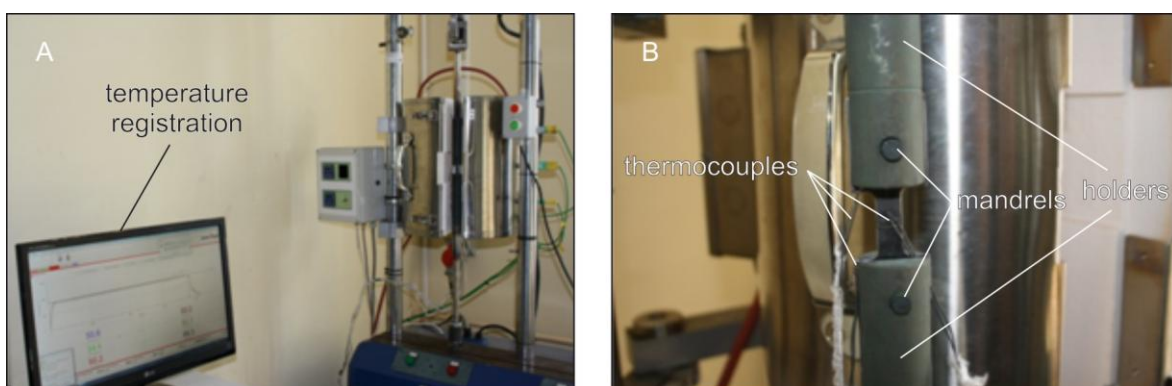


FIG. 3 — WPM ZST 3/3 CREEP TESTING MACHINE. A — A VIEW OF OPEN FURNACE WITH SPECIMEN MOUNTED IN HOLDERS BY MEANS OF MANDRELS; B — THE INSTALLED THERMOCOUPLES.

The creep tests were carried out as per standard [17] on WPM ZST3/3 (VEB Werkstoffprüfmaschinen Leipzig) creep testing machine equipped with three-zone LAB TEMP (Thermcraft Incorporated, USA) heating furnace operating at maximum temperature of 1200°C. 3 specimens were prepared and tested for each of the welding methods and each sheet metal thickness, for material both without and after heat treatment.

Fig. 3 shows a view of the creep testing machine with mounted specimen and three thermocouples attached along its length.

2.1 Preparation of metallographic sections for structural examination

Metallographic inspection (examination of microstructure and macrostructure) of welded joints made on 0.5-mm, 0.9-mm, and 1.2-mm thick sheet was carried out on metallographic sections prepared before and after heat treatment. The sections were obtained by means of mechanical polishing of transverse sections of the joints and etching with Kalling's reagent. Images were taken by means of Neophot 2 metallographic optical microscope equipped with advanced image acquisition and analysis system Multiscan V.08 and scanning electron microscope (SEM) VEGA 3 (Tescan) coupled with X-ray microanalysis adapter INCA x-art (Oxford).

III. RESULTS

3.1 Metallographic examination

Metallographic examination included observations of macrostructure and microstructure of welded joints made on thin Inconel 718 sheet specimens in as-delivered condition (not treated thermally) and after heat treatment. Revealing the macrostructure of joints was necessary to assess its shape, adjust the technological processes of GTAW and laser welding, and check the welds for possible presence of hot cracks.

3.2 Macrostructure of welded joints on sheet metal in as-delivered condition and after heat treatment

Examples of macrostructure observed in welded joints on thin Inconel 718 sheet in as-delivered condition made with the use of electric arc and laser are presented in Figs. 4–6, while Fig. 7 shows the microstructure after heat treatment.

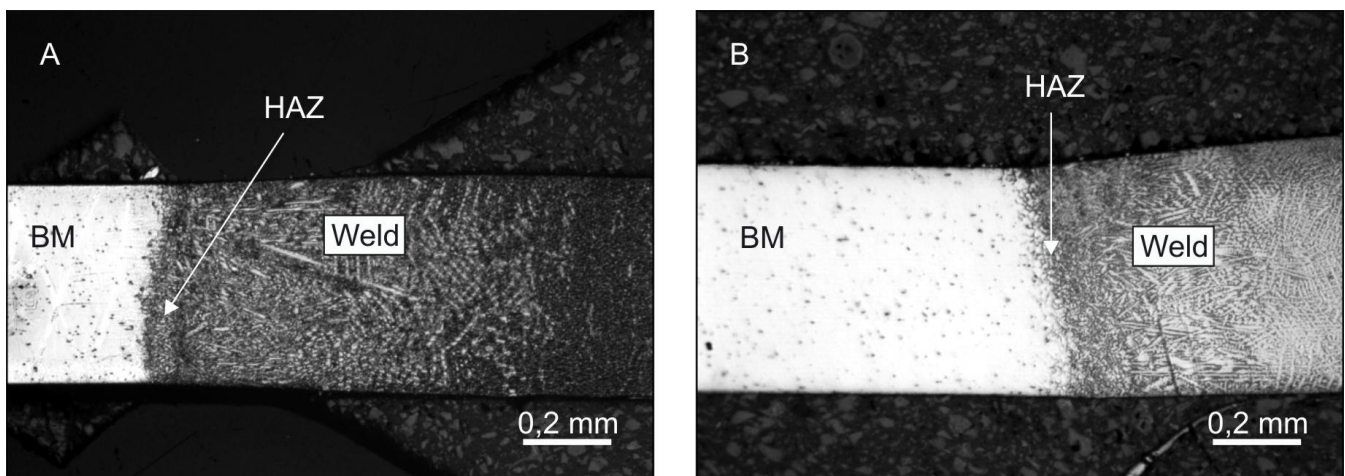


FIG. 4 — MACROSTRUCTURE OF A JOINT ON 0.5-mm THICK SHEET METAL MADE WITH: A — ELECTRIC ARC; B — LASER. VISIBLE ARE: THE WELD, HEAT-AFFECTED ZONE (HAZ), BASE MATERIAL (BM).

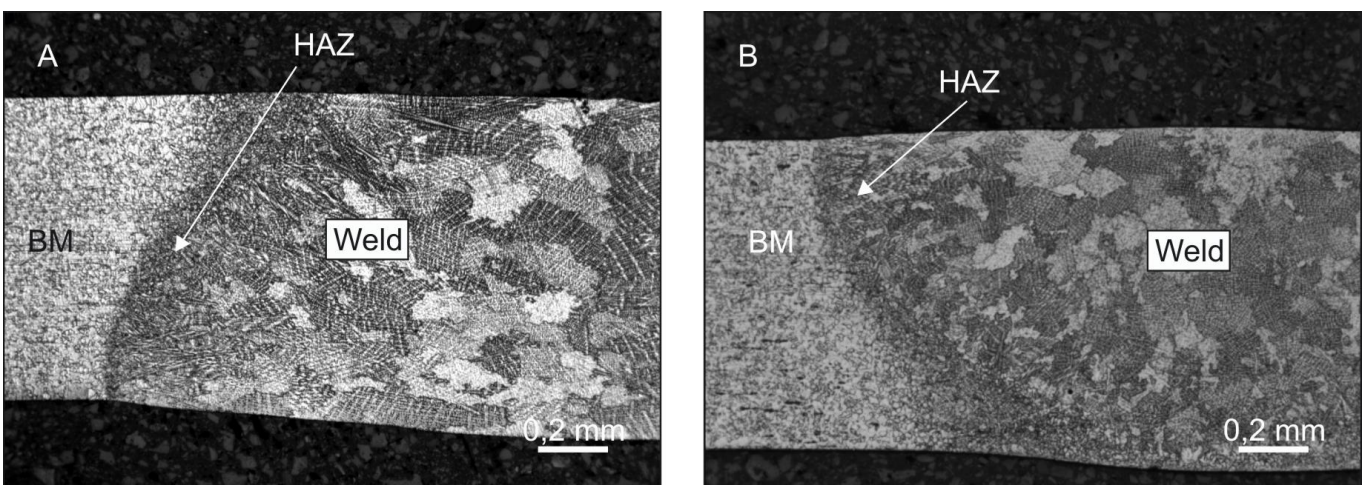


FIG. 5 — MACROSTRUCTURE OF A JOINT ON 0.9-mm THICK SHEET METAL MADE WITH: A — ELECTRIC ARC; B — LASER. VISIBLE ARE: THE WELD, HEAT-AFFECTED ZONE (HAZ), BASE MATERIAL (BM).

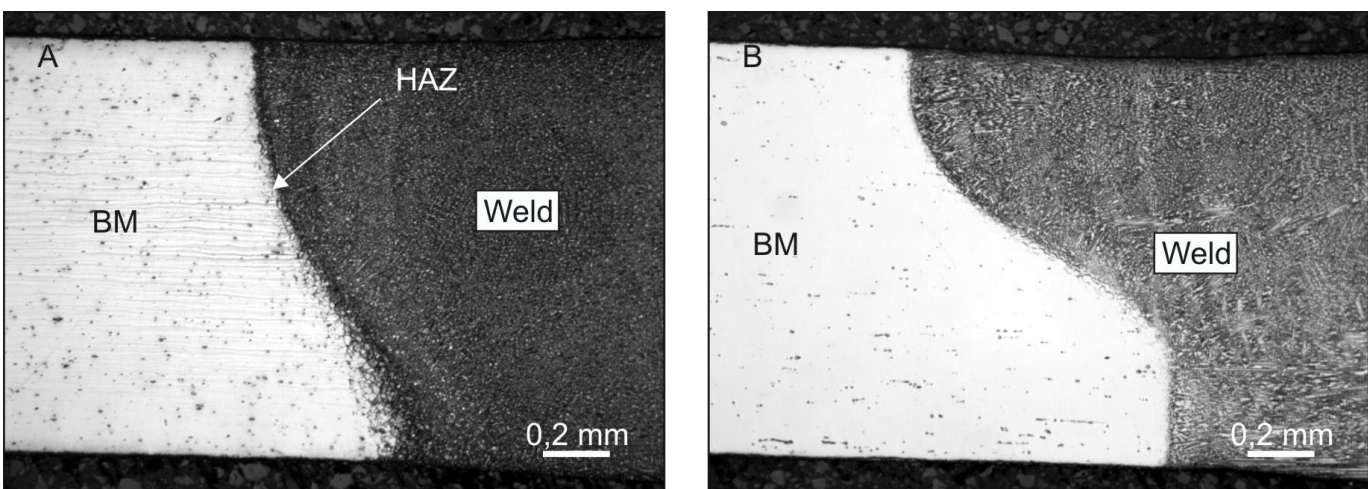


FIG. 6 — MACROSTRUCTURE OF A JOINT OF 1.2-mm THICK SHEET METAL MADE WITH: A — ELECTRIC ARC; B — LASER. VISIBLE ARE: THE WELD, HEAT-AFFECTED ZONE (HAZ), BASE MATERIAL (BM).

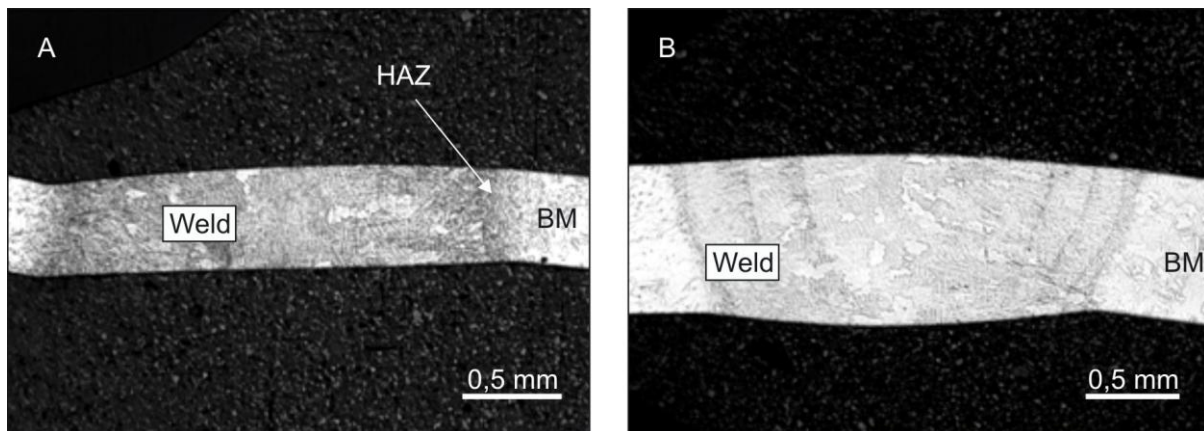


FIG. 7 — MACROSTRUCTURE OF A LASER-WELDED JOINT OF: A — 0.5-mm; B — 0.9-mm THICK SHEET METAL AFTER HEAT TREATMENT. VISIBLE ARE: THE WELD, HEAT-AFFECTED ZONE (HAZ), BASE MATERIAL (BM).

In thin sheet metal joints obtained with the use of different sources of concentrated heat streams, i.e. electric arc and laser light beam, one can distinguish between three characteristic structures: the weld, the heat-affected zones (HAZs), and the base material (BM).

Grains in welded joints have different morphology (shape and size) depending on welding method and parameters. Also the heat-affected zones of welded joints have different widths and grain sizes depending on the used welding methods and welding parameters such as current intensity, laser power, and welding rate.

3.3 Microstructure of welded joints on sheet metal in as-delivered condition and after heat treatment

Example result of microstructure examination of welded joints made on thin Inconel 718 sheet are presented in Figs. 8–11 for the material in as-delivered condition and in Fig. 12 for heat-treated specimens.

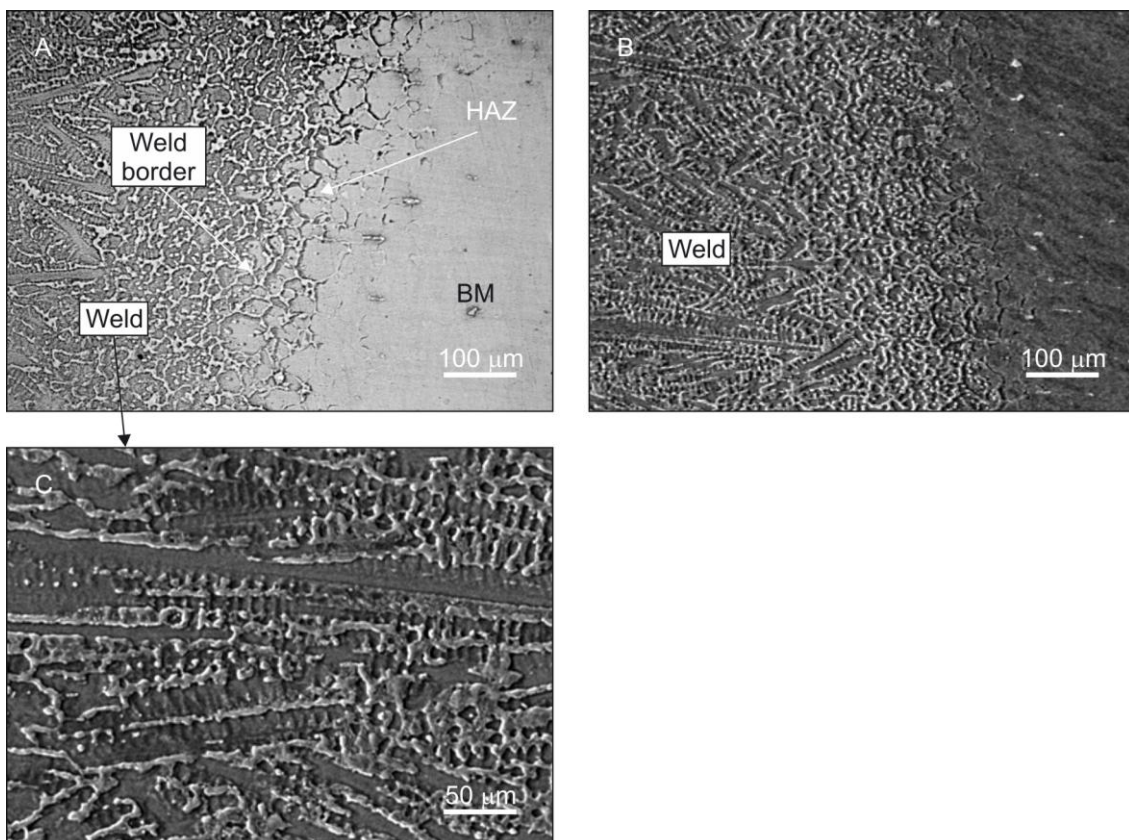


FIG. 8 — MICROSTRUCTURE OF AN ARC-WELDED JOINT OF 0.5-mm THICK SHEET METAL. A — OPTICAL MICROSCOPE; B, C — SEM.

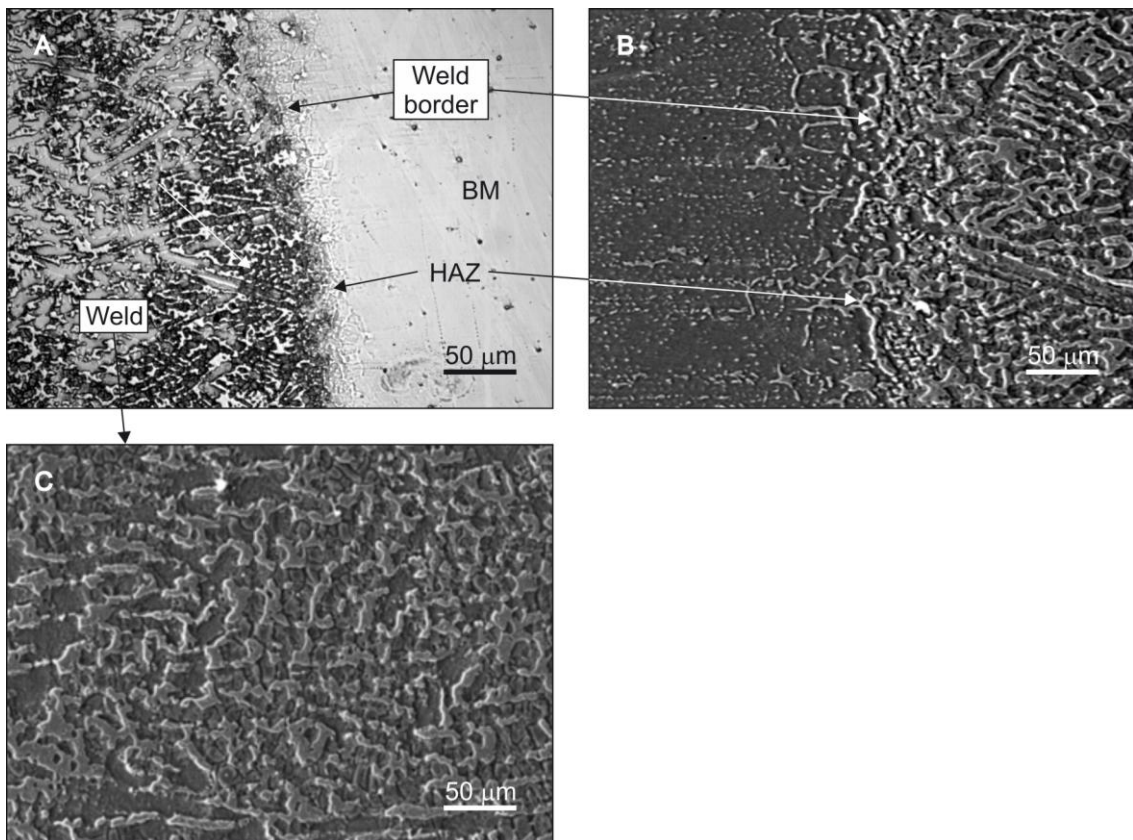


FIG. 9 — MICROSTRUCTURE OF A LASER-WELDED JOINT OF 0.5-mm THICK SHEET METAL. A — OPTICAL MICROSCOPE; B, C — SEM.

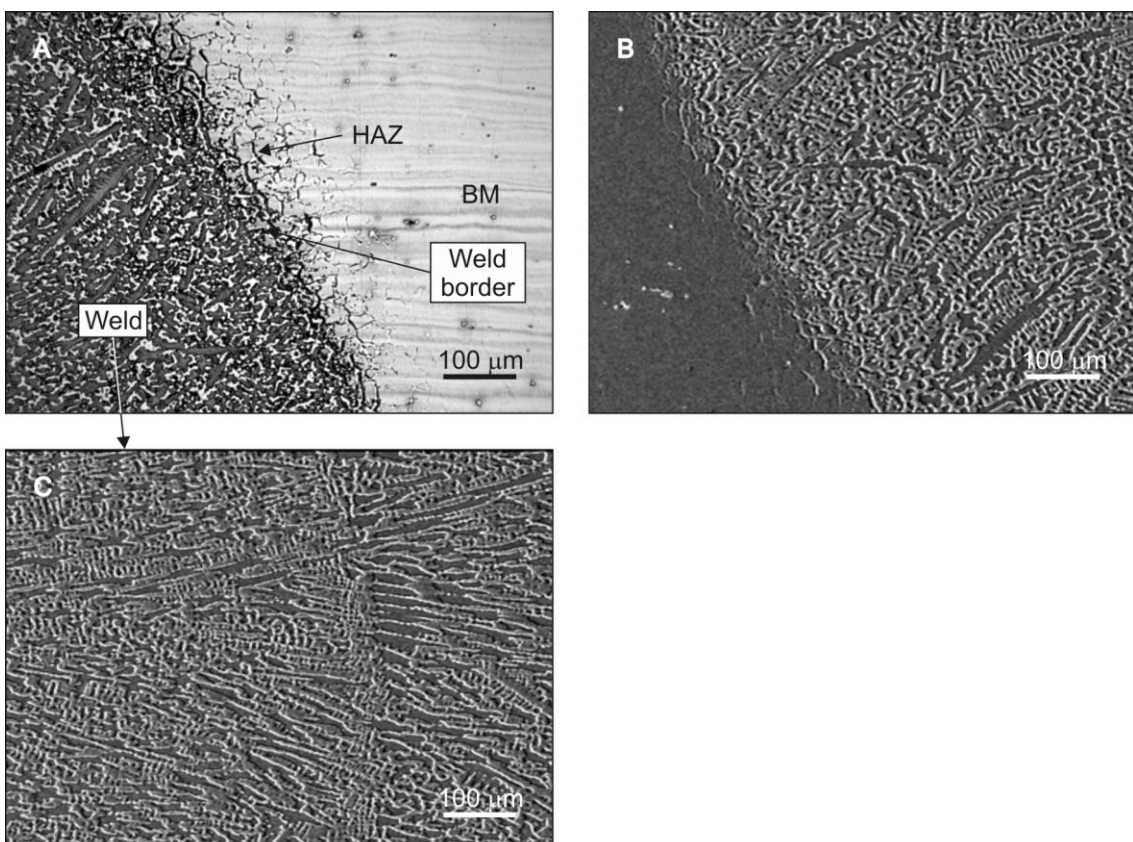


FIG. 10 — MICROSTRUCTURE OF AN ARC-WELDED JOINT OF 1.2-mm THICK SHEET METAL: A — OPTICAL MICROSCOPE; B, C — SEM.

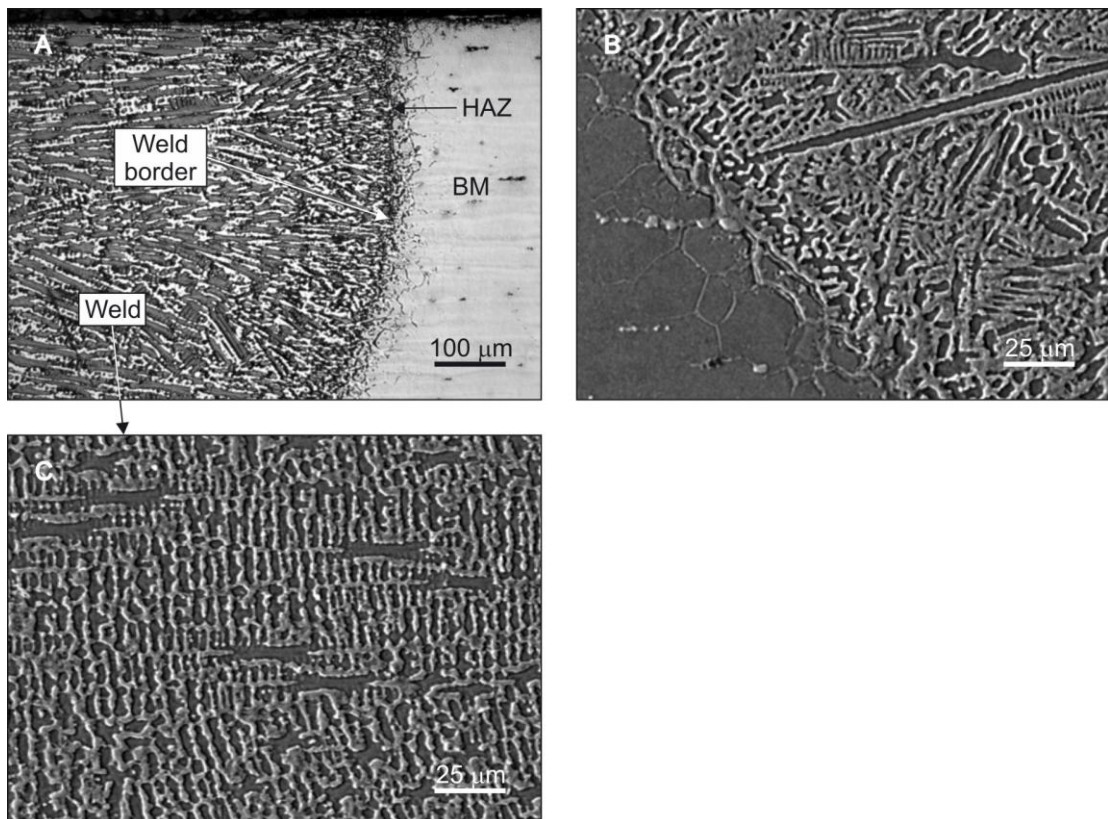


FIG. 11 — MICROSTRUCTURE OF A LASER-WELDED JOINT OF 1.2-mm THICK SHEET METAL. A — OPTICAL MICROSCOPE; B, C — SEM.

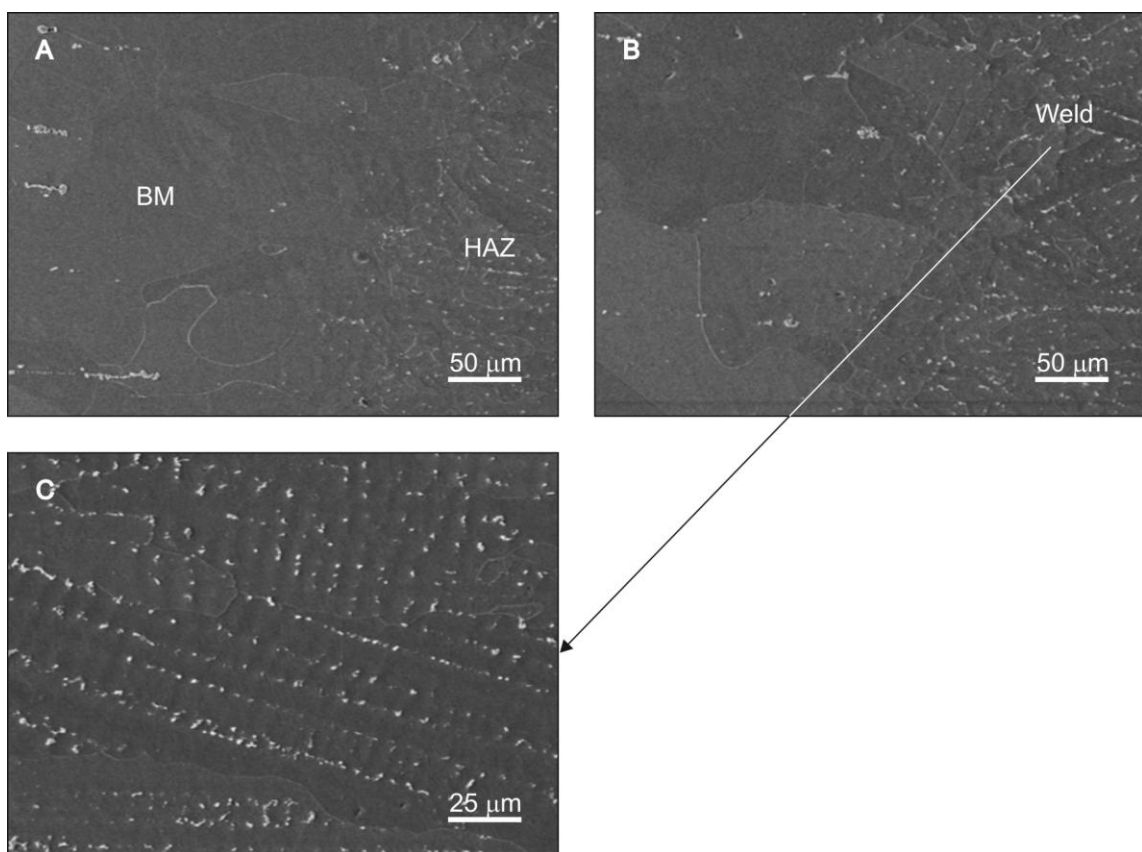
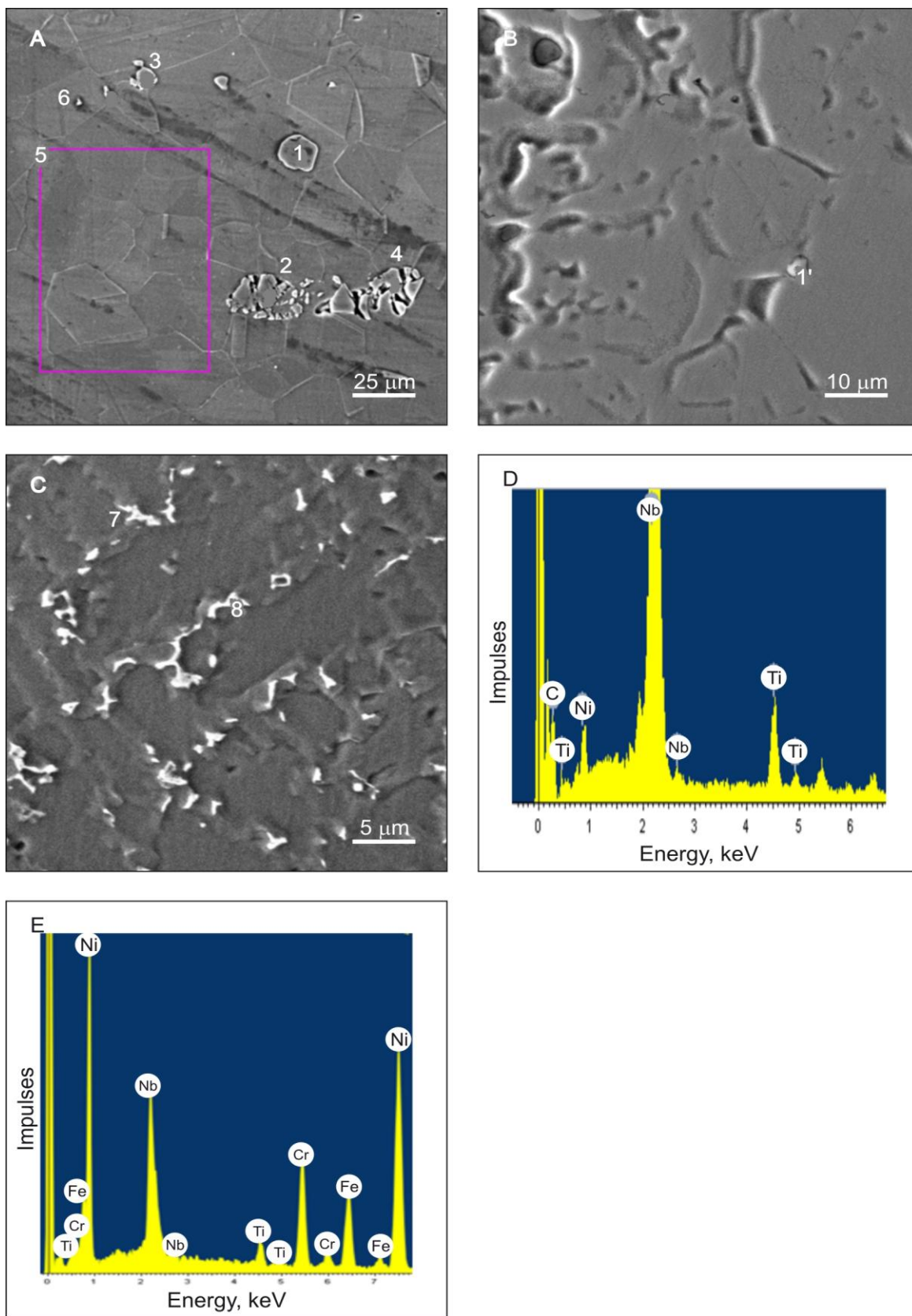


FIG. 12 — SEM IMAGES OF MICROSTRUCTURE OF A LASER-WELDED JOINT OF 1.2-mm THICK SHEET METAL

IV. X-RAY MICROANALYSIS

Example results of X-ray chemistry microanalysis carried on in micro-areas of welded joints on Inconel 718 sheet in as-delivered condition and after heat treatment are presented in Figs. 13 and 14, respectively.



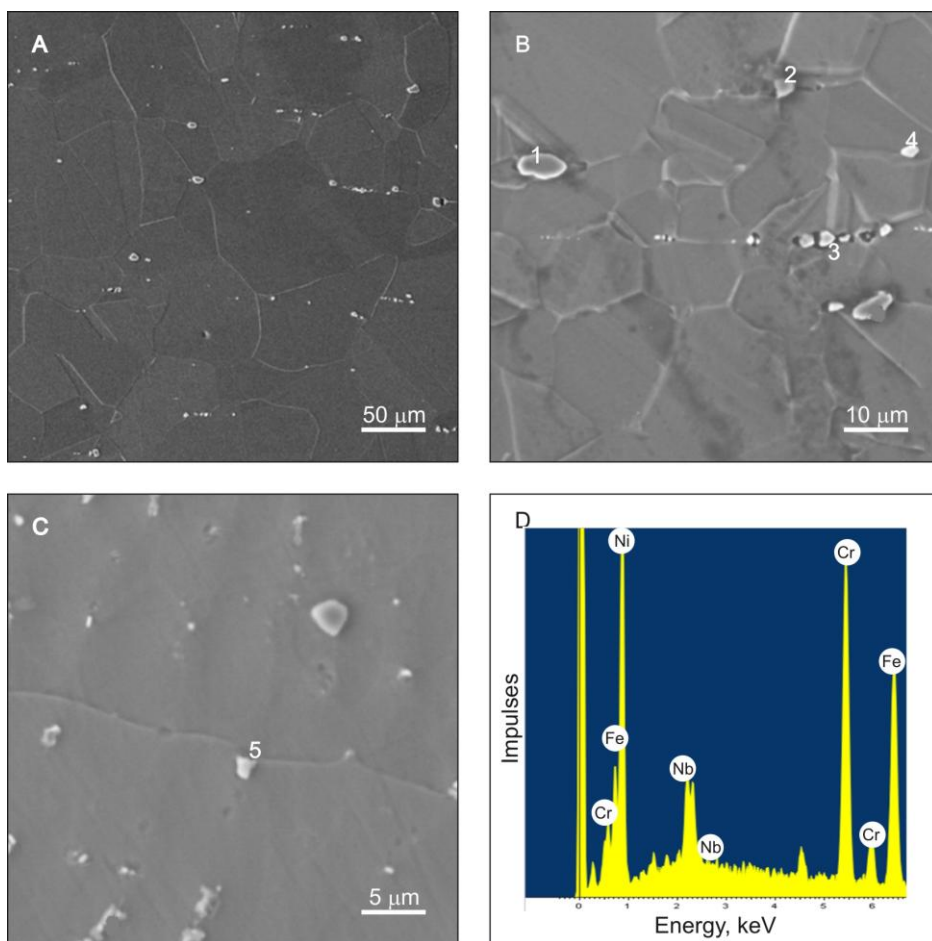
Micro-area No.	Element content (% wt.)						
	C	Ni	Nb	Cr	Fe	Ti	Mo
1	20.20 (64.0)*	1.70 (1.30)	70.80 (29.0)	—	—	7.30 (5.70)	—
1'	19.5	1.80	74.36	—	—	4.34	—
2	—	56.33	4.50	19.43	18.63	1.11	—
3	—	56.97	3.91	19.23	18.88	1.02	—
4	—	55.73	3.67	20.17	19.25	1.18	—
5	—	60.28	4.34	16.85	15.20	0.90	2.43
6	—	55.88	3.92	20.02	18.96	1.22	—
7	19.80	1.60	71.25	—	—	6.90	—
8	—	57.9 (55.7)	—	20.8 (22.7)	20.4 (20.6)	0.9 (1.0)	—

* Figures in parentheses denote element content in atomic %

FIG. 13 — MICROSTRUCTURE OF: A — BM; AND B, C — GTAW JOINT OF 0.9-mm THICK SHEET METAL IN AS-DELIVERED CONDITION WITH MARKED X-RAY MICROANALYSIS AREAS NOS. 1–8. ENERGY SPECTRA OF X-RAYS SCATTERED FROM: D — MICRO-AREA NO. 1; AND E — MICRO-AREA NO. 8. THE TABLE SUMMARIZES RESULTS OF X-RAY MICROANALYSIS.

Microstructure of Inconel 718 sheet in as-delivered condition reveals large grains of phase γ with carbides of MC type reach in niobium and titanium (Nb, Ti)C precipitated unevenly inside and on borders of the grains. Moreover, structure of the sheet metal contains irregular intermetallic phases rich in nickel, chromium, iron, niobium, and titanium. These are probably topologically close-packed (TCP) phases (σ phases). These phases correspond to compositions Ni(Cr, Fe, Nb) and Ni(Cr, Fe, Nb, Ti).

The seams in the joints welded both with electric arc and laser are characterized with dendritic structure. In welded joints of sheet metal in as-delivered condition, irregular eutectic composed of intermetallic phases (σ phases) and MC-type carbides is located on boundaries of phase γ dendritic grain branches.



Micro-area No.	Element content (% wt.)						
	C	Ni	Nb	Cr	Fe	Ti	Al
1	19.25 (58.60)*	2.85 (1.70)	69.74 (34.56)	—	—	8.16 (5.14)	—
2	—	50.50	3.50	18.05	16.99	1.15	0.64
3	—	56.80	4.57	19.71	18.92	—	—
4	—	55.74	4.07	19.98	19.27	0.94	—
5	—	53.2	19.8	12.7	12.1	2.2	-

* Figures in parentheses denote element content in atomic %

FIG. 14—MICROSTRUCTURE OF: A, B—BM; AND C—LASER WELDED JOINT OF 1.0-mm THICK HEAT-TREATED SHEET METAL WITH MARKED X-RAY MICROANALYSIS AREAS NOS. 1–5. D—ENERGY SPECTRUM OF X-RAYS SCATTERED FROM MICRO-AREA NO. 3. THE TABLE SUMMARIZES RESULTS OF X-RAY MICROANALYSIS.

In heat-treated sheet metal, the base material comprises equiaxial large grains of phase γ with regularly distributed (especially on grain boundaries) rounded MC-type carbides and residues of unsolved intermetallic phases (Fig. 14). Welded joints of heat-treated sheet metal have dendritic structure. It can be seen that irregular eutectic is almost completely dissolved in solid γ solution. On boundaries of phase γ grains' second-order branches there are finer rounded σ phases Ni(Nb, Cr, Fe, Ti) and spherical MC-type carbides rich in niobium.

4.1 High-temperature creep test

High-temperature creep tests were carried out at constant temperature on specimens prepared specifically for the purpose of this study out of Inconel 718 sheet with thickness 0.5 mm, 0.9 mm, and 1.2 mm (Fig. 2) with the use of creep testing machine (Fig. 3). Creep tested were specimens with welds made using GTAW method and with laser, untreated and heat-treated. Figs. 15 and 16 show example specimens ruptured in high-temperature creep tests.

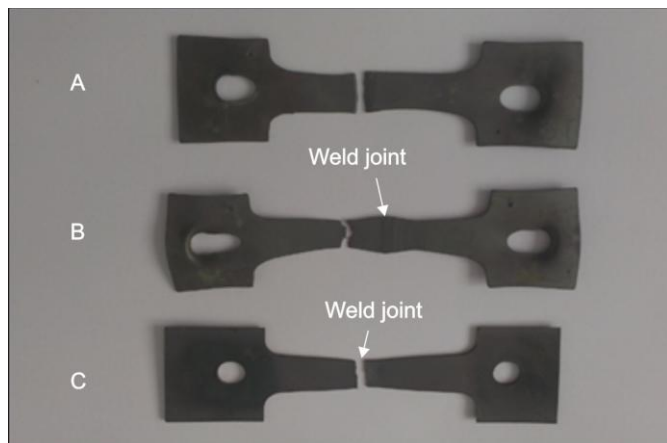


FIG. 15—EXAMPLE SPECIMENS OF 1.0 mm SHEET ALLOY IN AS-DELIVERED CONDITION RUPTURED AFTER HIGH-TEMPERATURE CREEP TEST. A—BM; B—LASER-WELDED JOINT; C—GTAW JOINT.

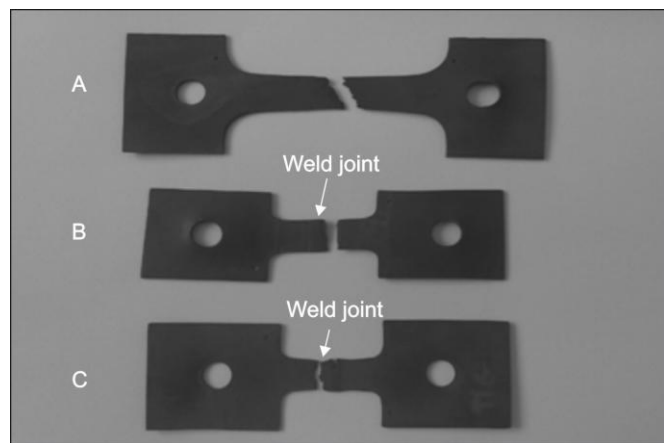


FIG. 16—EXAMPLE SPECIMENS OF 1.0 mm SHEET ALLOY, HEAT-TREATED AND RUPTURED IN HIGH-TEMPERATURE CREEP TESTS. A—BM; B—LASER-WELDED JOINT; C—GTAW JOINT.

Table 2 shows results of high-temperature creep test, and Fig. 17 presents values of the time to rupture for specimens of sheet metal in as-delivered condition, heat-treated, welded by means of GTAW method and laser-welded in the form of a bar graph.

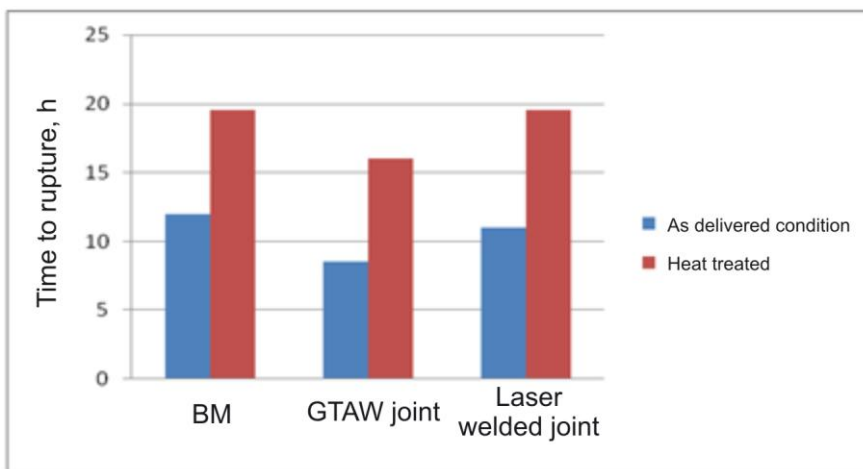


FIG. 17 — THE TIME TO RUPTURE MEASURED IN HIGH-TEMPERATURE CREEP TEST OF INCONEL 718 SHEET SPECIMENS. TEST CONDITIONS: $T = 860^{\circ}\text{C}$, $\sigma = 150 \text{ MPa}$.

The obtained results indicate that thin Inconel 718 sheet in as-delivered condition demonstrates a significantly shorter time to rupture in high-temperature creep tests than the heat-treated material. The welding method has significant effect on the time to rupture in the adopted high-temperature creep test conditions in case of sheet metal in both as-delivered condition and heat treated. Welded joints made with laser show the time to rupture values almost twice as high as those obtained for electric arc welding in argon atmosphere. Joints in Inconel 718 sheet specimens made with laser and heat treated demonstrate creep resistance similar to this of the base material (heat-treated sheet metal subject to high-temperature creep test).

When creep-tested at high temperatures, heat-treated Inconel 718 sheet specimens with GTAW joints got ruptured in the area of welded joints, just like those welded with the same method but in as-delivered condition. The joints made with the use of electric arc are characterized with lower creep resistance, and the time to rupture demonstrated by them in the high-temperature creep test has the value by about 30% lower than the time to rupture observed for sheet metal in as-delivered condition. GTAW joints of heat-treated sheet alloy show higher values of the time to rupture in the creep tests. The time to rupture value for sheet metal welded by means of GTAW and heat treated is similar to this characterizing base material without heat treatment (in as-delivered condition).

V. CONCLUSIONS

The initial material selected for the study were three grades of thin (0.5-mm, 0.9-mm, and 1.2-mm thick) sheet metal in as-delivered condition, rolled out of nickel-based Inconel 718 alloy. The material contained about 17% Cr, 16% Fe, 5.0% Nb, 2.5% Mo, 1.0% Ti, 0.60% Al, and 0.05% C. Total content of other elements such as Si, Mn, B, and N did not exceed 0.25%.

The microstructure of sheet metal reveals equiaxial grains of phase γ with dimensions of about $(100 \pm 15) \mu\text{m}$ with a small quantity of irregular phases σ and spherical carbides of MC-type sparsely distributed in the matrix. Intermetallic (TPC-type) phases σ have complex and diversified chemical composition (Fig. 13). These phases contain Nb and can be therefore described as Ni(Cr, Fe, Nb, Ti). There are also phases without Nb, Ni(Cr, Fe, Ti), as well as those without Ti, Ni(Cr, Fe, Nb). Carbides of MC type sparsely distributed in structure of the sheet metal contain mainly Nb and Ti and small quantities of nickel. They can be described as (Nb, Ti)C.

Thin Inconel 718 sheet in as-delivered condition with such microstructure shows good tensile strength on the level of about $(850 \pm 30) \text{ MPa}$ at high plasticity, and elongation on the level of $(30 \pm 3)\%$ [15]. The creep resistance of sheet metal in as-delivered condition determined by means of the time to rupture measured in high-temperature creep tests at temperature 860°C and under stress 150 MPa was 12 h at elongation of 48%.

Structure change induced by thermal treatment of Inconel 718 sheet consisting in solution treatment starting from temperature $1010^{\circ}\text{C}/8 \text{ h}/\text{H}_2\text{O}$ and two-stage ageing at temperatures $720^{\circ}\text{C}/8 \text{ h}$ and $620^{\circ}\text{C}/8 \text{ h}$ resulted in significant improvement of their strength properties. Tensile strength on the level of 1240 MPa was obtained with elongation similar to this measured for sheet metal in as-delivered condition [15].

Heat treatment (solution treatment and ageing) of Inconel 718 alloy sheet resulted in changes of morphological features characterizing its microstructure.

Mixtures σ -phase with diversified chemical composition irregularly distributed in the alloy's microstructure (Fig. 13) were almost entirely dissolved in solid solution of phase γ . Unsolved phase σ remaining in microstructure of Inconel 718 occurs on the form of fine rounded particles (Fig. 14). Similarly, MC-type carbides rich in niobium and titanium remaining in the alloy's microstructure have spherical shapes and are present in the form of fine particles on boundaries of γ phase grains.

It has been found that the current intensity I on the level of 80 A and the welding rate $V_s = 200$ mm/min were GTAW parameters most favorable from the point of view of thermal efficiency η_c and HAZ size. Such parameters of Inconel 718 sheet welding allowed to obtain good welded joints (Figs. 4–7) with minimum HAZ widths ranging from about 50 μm to 100 μm (Figs. 10–12).

Limited heat efficiency of laser light beam means that higher power levels must be used when welding thin Inconel 718 alloy sheet. Good joints on 0.7–0.9 mm thick sheet were obtained for laser with power of 400 W and welding rate of the order of 25 mm/s. For such laser welding parameters, the welded joints had virtually no HAZ (Figs. 4B, 5B, and 6B) or widths of their HAZs did not exceed 40 μm (Figs. 9 and 11).

The seams in the joints welded both with electric arc and laser reveal dendritic structure. Value of the structural parameter λ_{2s} characterizing dendritic grains of the joints depends on the welding method and decreases with increasing sheet metal thickness. In case of GTAW, increase of sheet metal thickness from 0.5 mm through 0.9 mm to 1.2 mm is accompanied by reduction of λ_{2s} parameter value from 12 μm through 10 μm to 8 μm . Similarly, in case of laser-welded joints, with sheet metal thickness increasing from 0.5 mm to 1.2 mm, λ_{2s} values decrease from 9.6 μm to 5 μm .

Boundaries of second-order branches of dendritic grains observed in welded joints on sheet metal in as-delivered condition made with the use of both GTAW and laser method are the locations where irregular eutectic (Fig. 13A) composed of σ phase and MC-type carbides can be found. Heat treatment (solution treatment and ageing) of welded sheet metal joints resulted in almost complete dissolution of σ phases and disappearance of irregular eutectic. On boundaries of joint grains' second-order branches there are fine rounded MC-type carbides surrounded with residues of σ phase (Fig. 14C).

A measure of creep-resisting properties of thin sheet Inconel 718 in as-delivered condition, heat-treated and welded with the use of GTAW and laser method is the time to rupture at adopted high-temperature creep conditions (Table 2, Fig. 17). The obtained results in combination with conclusions drawn from of microstructure examination of welded joints before and after heat treatment show that the use of laser welding allows to increase the time to rupture of heat-treated joints by nearly 62% in comparison with BM in as-delivered condition and by about 80% with respect to the time to rupture observed in GTAW joints made on sheet in as-delivered condition.

Specimens of sheet metal in as-delivered condition welded with the use of laser method and heat treated get ruptured outside the welded joint areas (Fig. 15B and 16B). It can be therefore concluded that laser-welded joints demonstrate higher creep resistance than the base material.

REFERENCES

- [1] Ruedl E., 1975 *Phase transformation in the alloy Hastelloy B*, Materials Research Bulletin 10, 16-22
- [2] Agarwal D.C., 2002 *Chronology of Developments in Ni-Mo Alloys: The Last 70 Years*, Corrosion 58, 27-29
- [3] Bloom D.S., Putnam J.W., Grant. N., 1952: Trans. AIME, *Journal of Metals* 194, 1, 626
- [4] Lancaster J., 1992: *Handbook of structural welding: processes, materials and methods used in the welding of major structures, pipelines and process plant*, Abington Publishing, Cambridge, 56-58
- [5] Hong J. K., Park J. H., Park N. K., Eom J. S., Kim M. B., Kang G. Y., 2008: *Microstructures and mechanical properties of Inconel 718 welds by CO₂ laser welding*, Journal of Materials Processing Technology, 1132-1138
- [6] Gozlan. E., Bamberger. M. S., Dirnfeld. F., Prinz. B., Klodt. J., 1991: *Topologically close-packed precipitations and phase diagrams of Ni-Mo-Cr and Ni-Mo-Fe and of Ni-Mo-Fe with constant additions of chromium*, Materials Science and Engineering A, 141, 85
- [7] Durand-Charne M., 1997: *The microstructure of superalloy*, Institut National Polytechnique de Grenoble, 48-52
- [8] Yukawa N., Hida M., Imura T., Kawamura M., Mizuno Y., 1972: *Structure of Chromium Rich Cr-Ni, Cr-Fe, Cr-Co and Cr-Ni-Fe Alloy Particles Made By Evaporation In Argon*, Metallurgy Transaction 3, 47
- [9] Klein J. H., Brooks C. R., Stansbury E. E., 1970: *The establishment of long-range order in NiCr using electron microscopy*, Physica Status Solidi 38, 831
- [10] Dupont J. N., Michael J. R., and Newbury B. D., 1999: *The weldability of an advanced corrosion-resistant alloy in investigated and linked to microstructural development in the fusion zone*. Welding Journal 78(12): 708-s to 415-s
- [11] Savage W. F., and Lundin C. D., 1965: *The Verestraint test*. Welding Journal 44(10): 433-s to 442-s

- [12] Savage W. F., and Lundin C. D., 1966: *Application of the Verestrain technique to the study of weldability*. Welding Journal 45(11):497-s to 503-s
- [13] Broks J. A., and Thompson A. W., 1991: *Microstructural deveploment and solidification craking susceptibility of austenic stainless steel welds*. International Materials Reviews 36: 16-44
- [14] Knorowski G. A., Cieslak M. J., Headley T. J., Roming A. D., and Hammelte W. F., 1989: *Inconel 718: a solidification diagram*. Metallurgical Transactions A 20 A:2149-2158
- [15] Jędrusik A., 2015: „*Technology of cutting, cleaning nad laser welding of thin sheet metal made of nickel alloy Inconel 718*” Doctor thesis, Rzeszow University of Technology
- [16] Opiekun Z., 2011: *Temperature influence of ceramic form on the structure of cobalt alloy MAR-M509 castings*. Acta Metallurgica Sinica (English letters) 24(1) 23-33
- [17] E-139-00 *Standard Test Methods Conducting Creep, Creep-Rupture, and Stress-Rupture Test of Metallic Materials*.